

New methods for ALMA angular-scale based observation scheduling, quality assessment, and beam shaping II: refinements

Dirk Petry^a, María Díaz Trigo^a, Rüdiger Kneissl^{b,c}, Ignacio Toledo^c, Atsushi Miyazaki^d, Toshinobu Takagi^d, Ashley Barnes^a, and Francesca Bonanomi^e

^aEuropean Southern Observatory, Karl-Schwarzschild-Str. 2, 85748 Garching, Germany

^bEuropean Southern Observatory, Alonso de Cordova 3107, Vitacura, Santiago, Chile

^cJoint ALMA Observatory, Alonso de Cordova 3107, Vitacura, Santiago, Chile

^dJapan Space Forum, 3-2-1 Kanda-Surugadai, Chiyoda-ku, Tokyo 101-0062, Japan

^eDept. of Astrophysics, University of Vienna, Türkenschanzstr. 17, 1180, Vienna, Austria

ABSTRACT

The Atacama Large Millimeter/submillimeter Array remains the largest mm radio interferometer observatory world-wide. It is now conducting its 11th observing cycle. In our previous paper presented at this conference series in 2020, we outlined a number of possible improvements to the ALMA end-to-end observing and data processing procedures which could further optimize the uv coverage and thus the image quality while at the same time improving the observing efficiency. Here we report an update of our results refining our proposed adjustments to the scheduling and quality assurance processes. In particular we present new results on ways to assess the uv coverage of a given observation efficiently, methods to define and measure the maximum recoverable angular scale, and on the robustness of the deconvolution in the final interferometric imaging process w.r.t. defects in the uv coverage. Finally we present the outline of a design for integrating uv coverage assessment into the control and processing loop of observation scheduling. The results are applicable to all radio interferometers with more than approx. 10 antennas.

Keywords: Radio Astronomy, Interferometry, Observatory Scheduling, UV Coverage, Image Fidelity

1. INTRODUCTION

The Atacama Large Millimeter/submillimeter Array (ALMA) is an international collaboration between East Asia, Europe, and North America in cooperation with the Republic of Chile. The official project website for scientists is the *ALMA Science Portal* <http://www.almascience.org>. A detailed description of ALMA and the standard terms and procedures mentioned here can be found in the Cycle 11 ALMA Technical Handbook¹ (THB). A brief introduction to the project and the issues we are addressing with this work, can be found in our first paper.² In order to avoid repetition, we assume in the following that the reader is familiar with ALMA observations and operations in general as they are described in the two references given above.

In this paper we present the results of an ESO ALMA internal development study on improving ALMA's methods of assuring the achievement of the science goals of its users both in observation scheduling and in subsequent quality assurance process (QA).

Further author information: (Send correspondence to Dirk Petry)
D. Petry: E-mail: dpetry@eso.org

2. THE BASELINE LENGTH DISTRIBUTION AS A TOOL IN SCHEDULING AND QUALITY ASSURANCE

In order to assess the sensitivity of an observation at all angular scales, we introduce the *Baseline Length Distribution* (BLD) in 1D (ignores baseline orientation) and 2D. The *observed BLD* of an ALMA observation (Member Observation Unit Set, MOUS, composed of one or more Execution Blocks, EBs¹) is the histogram of the baseline lengths (BLs) of the recorded interferometric visibilities for a representative channel in the representative spectral window and for a representative target *after removing invalid data* ("flagging"). Each entry is weighted by its integration time multiplied by the relative visibility weight (weight³ divided by the average weight for all baselines of the EB) and optionally by the squared ratio $(T_{sys,exp}/T_{sys,EB})^2$ of the expected system temperature $T_{sys,exp}$ and the actual average system temperature of all the antennas used in the EB. The unit of the histogram content is thus "visibility seconds" or "visibility hours" (see, e.g., Fig. 1).

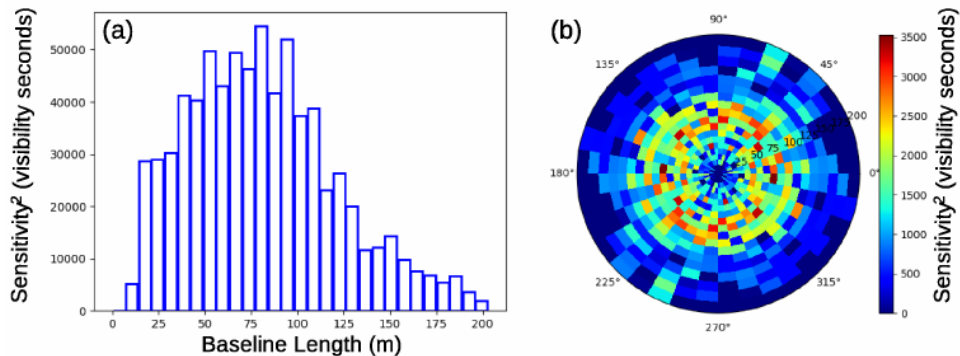


Figure 1. Example of a 1D Baseline Length Distribution (BLD) (a) and a 2D BLD (b), in this case for an 8 minute observation with the ALMA 12M array in a compact configuration.

The 1D BLD permits more clear visualisation, precise reading of values, and overplotting of different BLDs. However, only the 2D BLD contains all information for a complete uv coverage assessment, and we present here an assessment tool for full 2D treatment.

The principle investigator (PI) of an ALMA observation does not propose for a fixed observing time but defines "science goal" parameters for each MOUS which the observatory then aims to obtain in the most efficient way. An *expected BLD* can be derived from the science goal parameters Angular Resolution (AR), Largest Angular Scale (LAS), and sensitivity (translated internally into observing time) for the representative observation target. This BLD expectation can either optimise the Point Spread Function (PSF) shape or try to follow the typical BLD shape produced by the actual observatory, which uses a compromise between optimal PSF and being sensitive over a large range of angular scales.

Comparison of the observed and expected BLDs yields information about the BL range(s) where the MOUS lacks sensitivity and where it is overexposed. To quantify the differences, we introduce the *Filling Fraction* (FF) as the ratio of observed and expected visibility seconds in an individual BL bin. If the expectation is zero, the FF is defined to be unity to indicate that in the given bin no sensitivity is missing.

The weighting by $(T_{sys,exp}/T_{sys,EB})^2$ (mentioned above) needs to be applied to take into account sensitivity differences between individual EBs and between the actual and typical observing conditions. The FF for the entire uv plane (all BLs) then becomes equivalent to the "execution fraction" (EF) which ALMA has been using successfully since many Cycles to monitor the accumulated sensitivity and compare it to the planned total sensitivity of an observation.

Since we find that we need to separately assess PSF quality and fulfillment of scheduling goals, we use the term FF referring to the filling fractions derived from the expectation for optimal PSF, and the term EF referring to the filling fractions derived from the expectation for typical observatory BLD shapes.

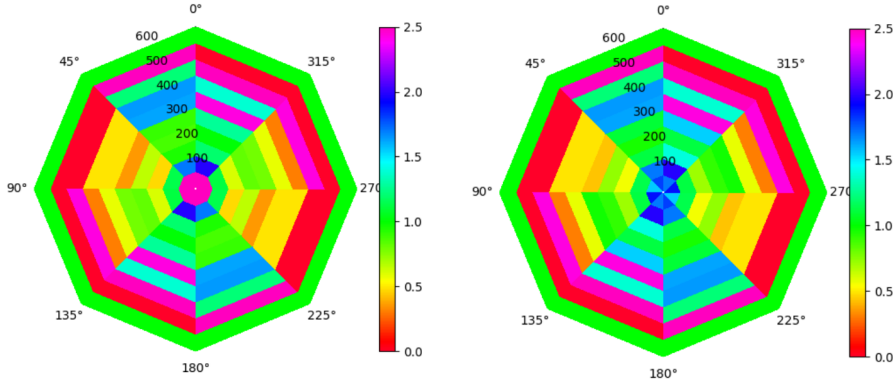


Figure 2. Example of 2D Filling Fraction (left) and Execution Fraction (right) plots for a case with sub-optimal uv coverage (a 24 minute observation with the ALMA 12M array with only 37 instead of normally at least 43 antennas in an intermediate configuration). There is underexposure (red, yellow) at the longest baselines in all sectors, and at intermediate baselines in one sector.

Computing the EF in separate regions of the uv plane permits to generalise the ALMA concept of the single-number EF, which was used in scheduling so far, and replace it by a matrix of values, the EF matrix. We recommend a 4×10 EF matrix in four azimuthal bins of 45° width and 10 equidistant BL bins between the shortest possible BL and the longest BL, where the latter is the maximum BL of the expectation or observation, whichever is larger.

A quality assessment can then be performed by defining conditions on the FFs and EFs. If the conditions are not fulfilled for a given MOUS, one can derive the array configuration and hour-angle range in which additional EBs should be scheduled to obtain the missing visibility seconds most efficiently. For multi-EB MOUSs, this procedure can already be applied in the first level of QA (QA0) to steer the scheduling of subsequent EBs.

2.1 Azimuthal uv coverage

It is important to note that achieving azimuthal completeness of the uv coverage and achieving the overall sensitivity in minimal time are two competing goals because optimal azimuthal coverage requires to make use of Earth rotation synthesis, even with the large number of antennas available to ALMA. For image quality, complete azimuthal coverage, i.e. having sufficient sensitivity for a given angular scale at all baseline *orientations*, is key. Achieving azimuthal completeness should therefore take precedence over minimizing the total observation time.

2.2 Maximum recoverable angular scale

The second pair of (in general) competing conditions is that of the achievement of the most Gaussian PSF for a given AR and achieving an arbitrary maximum recoverable angular scale (MRS). With the best PSF, the MRS of an ALMA 12M array with a given AR cannot be made much larger than ca. $8 \times \text{AR}$. To achieve larger values, the PSF has to be compromised and this is what was done in the design of the ALMA 43-antenna configurations (C43s). As mentioned above, we therefore need to distinguish between an expected BLD for best PSF and an expected BLD for the ALMA C43s.

2.3 Handling of mosaics

In a mosaic observation, each field (pointing) constitutes in principle a separate observation with its own uv coverage. However, since the time per visit to each field is chosen to be short compared to the total observing time spent on the mosaic, the difference which Earth rotation causes between the uv coverage patterns achieved for each individual field should be small.

Our new uv coverage assessment procedure includes the generation of a diagnostic plot to confirm this: the BLD for each mosaic field is measured separately and all BLDs are put in one plot such that differences between the uv coverage of the individual pointings are immediately obvious. We find that for the ALMA 12M array,

the deviations between the individual BLDs of the mosaic fields are in general smaller than 1% such that an assessment of the average BLD (over all fields) or simply the sum of the BLDs over all fields of a mosaic is a valid test of the uv coverage quality.

3. IMPACT OF BLD DEFECTS ON THE IMAGING RESULTS

In order to decide on the tolerances within which the expected BLD is to be achieved by an ALMA observation, we have studied the consequences of non-ideal BLDs on the image quality and the derived scientific results.

3.1 Recovery of parameters of Gaussian-shaped objects

We initially examined simulated 12M array observations of a complex test image with groups of Gaussian blobs at a large range of angular scales (Fig. 3 a, b, c). We found that the results of the standard imaging process with CASA `tclean`³ are only weakly deteriorated by deviations of the BLD from the ideal *as long as a significant sensitivity to all relevant angular scales is maintained*. We determined that at least 77% of the ideal sensitivity (corresponding to FF= 50%) needs to be retained at each angular scale range in order to keep image quality indistinguishable from that achieved with the ideal BLD.

3.2 Simulation and analysis of stylised proto-planetary disks

In order to study a more complex target shape than a Gaussian, we created test images for each standard ALMA C43 containing concentric rings with dimensions ranging from close to the configuration’s angular resolution to its maximum recoverable scale as given by the ALMA THB.¹ This setup is meant to resemble a stylised ”proto-planetary disk”, one of the typical targets of ALMA. To challenge the deconvolution, the setup was studied with and without a bright compact source close to the edge of the outermost ring (Fig. 3 d, e, f).

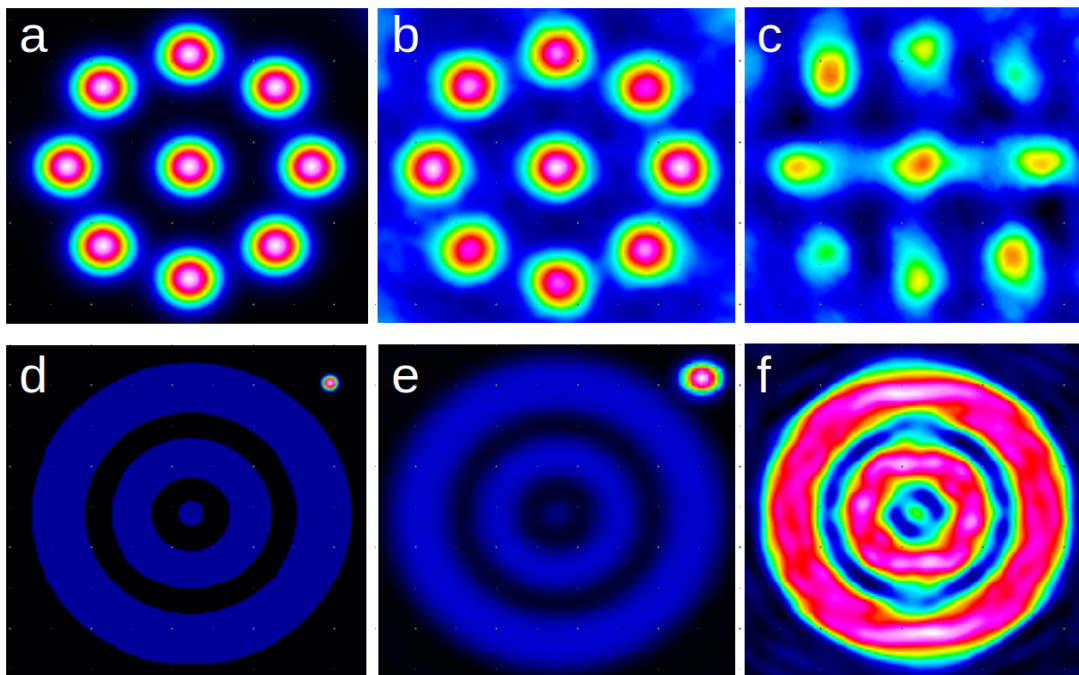


Figure 3. Illustrations of the two different sub-studies performed to measure the impact of BLD defects on image quality via simulations: (a) synthetic pattern of Gaussians used as input for an ALMA observation simulation, (b) result of the simulated observation of (a) with a BLD of near-ideal shape, (c) like (b) but for a non-ideal BLD, (d) synthetic pattern to be used as input for an ALMA observation simulation resembling a protoplanetary disk with a nearby bright compact source, (e) result of the simulated observation of (d) for an ideally shaped BLD, (f) similar to (e) but with a non-ideal BLD and without the bright source to make details of the structure recovery more visible.

Varying the BLD of the simulated array, we found again that the imaging process is very robust to BLD defects until they begin to become larger than 40% over a range of ca. 20% of the overall BL range. But only when defects of 80% (i.e. FF=20%) are introduced in this way, do the corresponding deviations of the measured image parameters (like ring gap size, over-all flux etc.) become severe. This argues for a general lower limit on the FF of 25% corresponding to placing the upper limit on the acceptable noise RMS in a given uv coverage bin to *twice* the expected value.

Here and also in the general measurement of the MRS for the standard ALMA configurations, we find that it is important to monitor the homogeneity of the azimuthal coverage especially for the shortest baselines. Generally, missing azimuthal coverage in a given BL range can cause very misleading image artifacts if the observed object is bright at the corresponding angular scales. The impact on general image fidelity is particularly large when bright extended objects are observed with incomplete (but not absent) uv coverage at the short baselines.

3.3 Full astrophysical modeling of a real protoplanetary disk observation

We used code provided by T. Paneque-Carreño⁴ to fit a well-tested model of protoplanetary disk structure to an ALMA dataset following a published procedure. By again varying the BLD of the input dataset while keeping the overall sensitivity constant, we test how the fit results for the four model parameters react to the different BLD defects. Fig. 4 shows examples of the changes which the defects cause in the image cube, while Fig. 5 shows examples of the impact of these changes on the model parameters.

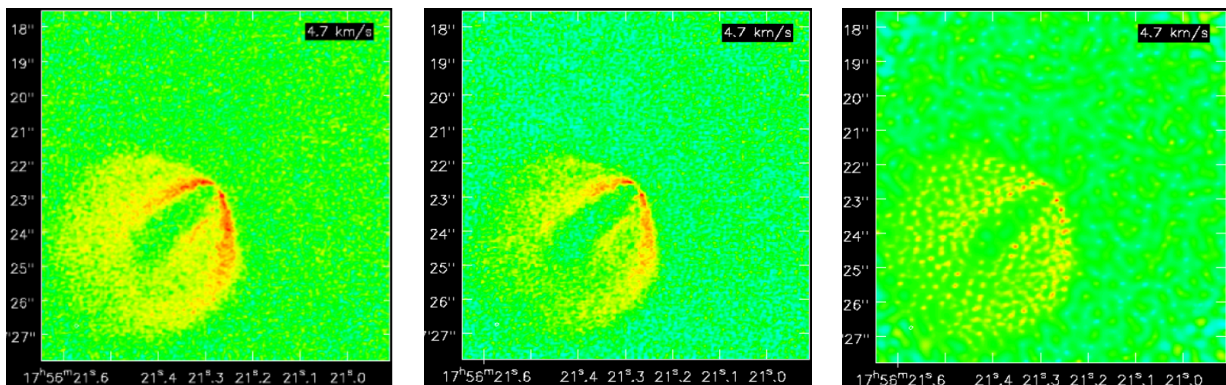


Figure 4. Narrow bandwidth (single-channel) image of the emission from a protoplanetary disk with different modifications to the BLD of the dataset before imaging: (left) ideal BLD, (middle) redistribution of sensitivity to remove 60% of the visibilities from the lowest 10% of the BLD, (right) redistribution of sensitivity to remove 80% from the lowest 10% of the BLD. All three datasets have the same sensitivity when integrating over all angular scales.

Here we find that defect sizes of ca. 50% are the tolerable limit. At this point, the parameter variations are as large as the statistical errors given by the fit algorithm. At a defect size of 80%, the change caused by the introduction of the BLD defect, in particular in the lower half of the BL range, can be several times larger than the nominal statistical error and thus unacceptable. The instrument is then simply no longer sensitive to the angular scales which dominate the emission from the protoplanetary disk. This again argues for implementing at the very least a lower FF limit of 25%. Each BL range (averaged over azimuth) should contain at least 50% of the expected visibility seconds, i.e. have $FF \geq 50\%$.

3.4 Other considerations and conclusions

The deconvolution process using the CLEAN algorithm³ is able to repair shortcomings of the BLD, i.e. shortcomings of the PSF, sufficiently well unless the angular scale and orientation in question is sampled with significantly lower sensitivity than the rest of the BLD.

The exact limit to the tolerable BLD defects may depend on the science goal, but our results show consistently that the deformation of the BLD away from the ideal shape by ca. 50% in a range with a width of 20% of the

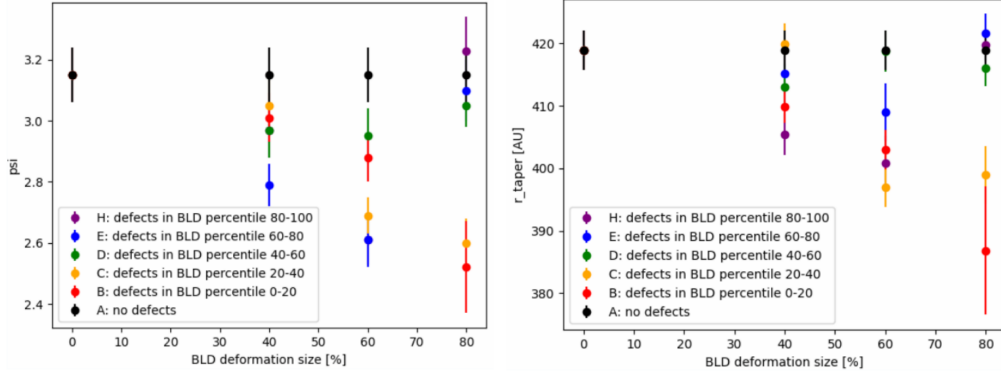


Figure 5. Fit results on the different imagecubes from a CO line observation of a protoplanetary disk obtained with the ideal BLD (case A, black) and deformed BLD (cases B, C, D, E, H, other colours) plotted as a function of the defect size. **Left:** fit result for the parameter ψ . **Right:** fit result for the parameter r_{taper} . The two parameters control the exponential decay of the altitude of the emitting surface of the protoplanetary disk over the plane of the disk as a function of radial distance from the disk center. The error bars shown represent the statistical errors provided by the fitting routine. As one can see, from a defect size of ca. 50% onwards, the systematic errors caused by the BLD deformation dominate over the statistical errors.

total baseline length range* is the point beyond which the effects on the scientific results of the observation become significant and need to be included as additional systematic errors.

Our results show furthermore that a BLD underachievement by 75% (50% in sensitivity) in a given angular scale range seems to be the maximum acceptable defect for an observation of an object with emission in that angular scale range. Observations with defects beyond this size need special analysis techniques and can no longer be imaged in the conventional way.

Further arguments for keeping the BLD close to the ideal for a Gaussian PSF are the following:

1. A Gaussian PSF minimizes the noise-correlation in an interferometric image.⁵
2. A Gaussian PSF minimizes the systematic errors on flux recovery.⁶
3. A Gaussian PSF minimizes the computing time needed for deconvolution since the flux to be redistributed in the image by the deconvolution process is minimal. An observation performed with a perfectly Gaussian beam would require no deconvolution at all.⁷

4. COMPUTING THE EXPECTED BLD

The ideal shape of the BLD can be derived from conditions on the shape of the PSF of the interferometer and on the sensitivity at large angular scales. These conditions concern (a) the FWHM of a Gaussian fit to the PSF (corresponding to the achieved AR or smallest resolved angular scale), (b) the LAS (Largest Angular Scale of the science target) or the MRS of the observation, and (c) the requirement of a general Gaussian shape of the PSF with minimal negative bowls.

We have studied two methods to compute a BLD from the AR and MRS and find that our "analytical" method is the preferred one² since it agrees in most BL ranges with the present design of the ALMA configurations and is optimised for a Gaussian PSF. The "analytical" method computes the 2D BLD as a 2D Gaussian with an inner taper and then derives the 1D BLD.

The MRS which the "analytical" BLD can achieve is, however, limited to ca. $8 \times \text{AR}$. As mentioned above, we therefore need to introduce a *modified analytical expectation* which can achieve the MRS values typically

*which corresponds to a loss of roughly 23% in sensitivity in that range and an equivalent gain in the remaining ranges since we are keeping the overall sensitivity constant

requested from ALMA. This expectation is closer to the shape of the C43 configurations because the design of these configurations followed the same reasoning. It differs from the "analytical" BLD only in the lowest 10% of the BL range and at intermediate BLs near the peak of the BLD.

An alternative method for computing an expected BLD is what we call the "filled dish" (FD or "simulation") approach.² It fills a 2D aperture of a diameter corresponding to the AR with randomly placed antenna positions imposing a minimum distance between all antennas corresponding to the MRS. We do not recommend to use this method for the ALMA 12M array but we intend to study it further since it seems to have potential for BLD assessment in observations with data combination between different 12M arrays and also for the ALMA 7M array. The difference in BLD shape w.r.t. our first ("analytical") method consists mainly in a stronger emphasis on longer baselines with a cutoff at the BL which corresponds to the AR. Furthermore, the FD method permits to extrapolate in a simple way to zero BL and may thus be helpful in judging the BLDs of combined 12M array, 7M array, and single-dish (non-interferometric) datasets when pseudo-visibilitys are introduced for the single-dish data. Filled-dish array configurations have been studied in the past⁸ and found to perform well.

The main reason why we recommend the "analytical" method over the FD method is that a pure FD BLD cuts off abruptly at a certain maximum BL and thus does not optimize the side-lobe level, in disagreement with the present ALMA 12M configuration design.

5. PROPERTIES OF THE BLDs OF REAL ALMA OBSERVATIONS, MRS MEASUREMENT, AND THE TM1+TM2 SCHEME

5.1 Underexposure at intermediate baseline lengths in the ALMA data

From our study of nearly 500 Cycle 6 and 7 and ca. 250 Cycle 9 12M MOUSs, we find that the ALMA 12M array observations show in general enough sensitivity at large and small angular scales but fall short of the requirements for an ideal PSF at *intermediate* scales. This is true regardless of the exposure time, the target elevation, and the number of antennas used. This is just a confirmation of what we have seen in simulations in the nominal C43s, although there are significant differences among the configurations, with the compact ones being closer to the ideal[†] and the more extended configurations deviating more significantly from it. As mentioned above, this is a consequence of the intention of the designers of the C43s to keep some large scale coverage while increasing sensitivity to shorter scales, all with the same total number of antennas. Furthermore, some compromises with antenna relocation management were necessary.

5.2 Exposure at the shortest baselines, MRS measurement, and implications for TM2

The C43 design results in an overexposure of most MOUSs at the shortest baselines compared to our "analytical" expectation of the BLD shape. This means that (a) on the MOUS level, the PSF shape of this data is sub-optimal and (b) on the GOUS level, i.e. when combining several 12M array observations from different configurations to achieve large angular scale coverage, at least the TM1+TM2 array combination groups have an even less optimal PSF because here a TM2 (compact-configuration) observation is added to a TM1 (extended-configuration) observation to match a large requested MRS, which mostly increases the sensitivity at short baselines where the deviation from an ideal BLD shape is already large.

We looked further into the question of scheduling and assessing the uv coverage at short baselines by first developing methods to define and measure the MRS in a more stringent way.

5.2.1 MRS and AR measurement via the "Flat sensitivity" plot

Following a suggestion by Ryan Loomis (NRAO), we developed a new tool to compare the achieved sensitivity in a given BL range to an ideal, constant sensitivity over the entire observed angular scale range. This approach is related to methods developed for the analysis of the CMB.⁹ Based on information-theoretical considerations, the ideal of a sensitivity independent of angular scale is what an observer may naively assume when looking at an interferometric image.

[†] "ideal" here refers to our recommended "analytical" method of computing the BLD expectation

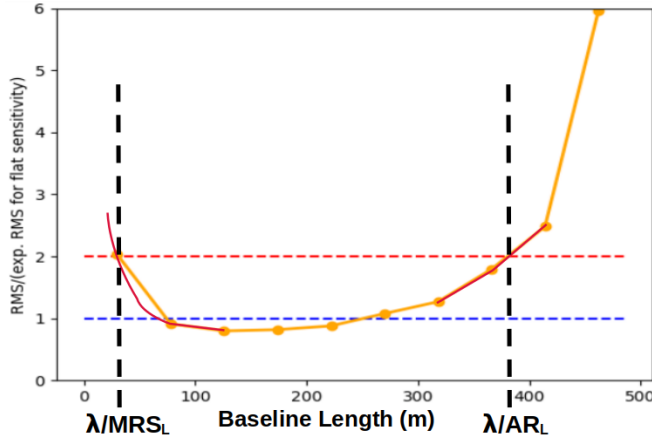


Figure 6. Example of a "flat sensitivity" plot for a Cycle 9 observation of 6 min on-source time with the ALMA 12M array with 46 antennas in an intermediate configuration. The red curves indicate parabolic fits to the three points closest to the intersections with the red line of constant value 2.0 . The baseline lengths corresponding to these intersections are used to define the values of MRS_L and AR_L . See text.

The expected level of sensitivity in each BL bin of the BLD is determined such that the sensitivity is constant over the entire accessible angular scale range in bins of equal width *in angular scale* and the overall sensitivity is equal to the observed one. Plotting the ratio of the actually achieved and the thus expected noise RMS in each BL bin versus BL gives a typically U-shaped graph indicating that in the middle of the observed BL range, the achieved noise RMS is better than expected, and at the lower and upper end of the BL range the noise RMS diverges. We call this plot the "flat sensitivity" plot. Fig. 6 shows an example.

This plot permits to define the maximum recoverable scale MRS_L as the angular scale corresponding to the shortest BL where the achieved noise RMS is still smaller or equal to the max. acceptable RMS. We choose the max. acceptable noise RMS as $2 \times$ the expected RMS based on our results in section 3. In our plot of the noise RMS ratio this means that the MRS_L corresponds to the smallest BL where the plot reaches a value ≤ 2 . Similarly, also an AR can be defined as the angular scale corresponding to the *largest* BL where the RMS is still $\leq 2 \times$ the expectation. We call this the AR_L .

Studying real data from Cycle 9 and simulations of all C43s, we find that AR_L is well correlated with and on average equal to the standard measurements of AR via PSF analysis during image deconvolution.

The agreement of the MRS_L with the MRS values derived from the L05 (as described in the THB) is equally good both when measured in simulations and in real Cycle 9 data.

5.2.2 Measurement of the MRS via imaging and flux recovery

The MRS values in the ALMA THB were obtained by analysing the Fourier transforms of uniformly filled disks and determining at which BL they drop below 10% of the theoretical maximum amplitude, the total flux of the disk, i.e. by identifying the approximate position of the first minimum in the *sync-function-like* Fourier transform of the uniform disk.¹⁰ This method is not intuitive for general ALMA users who think of their observation targets in terms of all angular scales *combined*.

To provide an alternative measurement, we set up snapshot (3 min per field, 60 min total) simulated small mosaic observations of (a) Gaussian objects and (b) uniform disks of different sizes. We vary the FWHM of the Gaussian (or the diameter of the disk respectively) from a few times the THB AR value of the configuration to several times the THB MRS value. We then image the resulting simulated visibilities with standard CASA "tclean" procedures³ and measure the total flux of the object image. Finally, we measure the flux recovery ratio as a function of object size and define the MRS as the FWHM of the input Gaussian (or as the diameter of the disk) for which the flux recovery drops below a certain limit, e.g. 50%. We find that this alternative way of

measuring the MRS results in systematically larger values than those given by the THB. In particular for the disks, we obtain MRS values which come close to the theoretical limit of the MRS which is λ/BL_{min} .

For the Gaussians, we obtain MRS values which are closer to but still mostly above our MRS measurements from the "flat sensitivity" plots (MRS_L), which are themselves consistent with the MRS values derived from the L05 following the THB.

In order to investigate the dependence of the MRS on noise level, we also study a low SNR case for the Gaussians which demonstrates that there is a significant deterioration of MRS value when going from a dynamical-range-limited case to a peak SNR of only 20.

All our MRS values are conservative since they are based on simulations at the elevations of ca. 85° . Observations at lower elevations will have at least partially foreshortened baselines due to the projection effect and so the shortest baselines will be up to a factor $\sin(\text{elevation})$ shorter than their nominal length, but never shorter than the dish diameter (because of shadowing). This will correspondingly raise the MRS. The exact value will depend on the hour-angle distribution and the Declination of the object.

On average, our MRS derived from the flux recovery in high-SNR simulations of Gaussians is a factor 1.5 larger than the THB reference value, while the value derived from low-SNR simulations is only a factor 1.36 larger.

In ALMA Cycle 9 data, we find that 97% of the studied representative sample of single-MOUS observations have achieved the requested LAS.

5.3 General overexposure

In general, the sensitivity reached in ALMA observations up to Cycle 9 was often significantly better than requested. So methods to improve the BLD shape during offline analysis could be applied without the overall sensitivity dropping below the requested value. We have produced prototype code to demonstrate the adjustment of the BLD by re-weighting but have to leave a detailed examination of the trade-off between improvement in PSF shape and loss in sensitivity to the future.

In cases of bright objects, this approach looked particularly promising for 7M data which can have bad PSF shapes due to the 7M array's small number of baselines. But first tests of the concept did not give good results. The 7M array is lacking baselines of 40 m - 70 m length to obtain a reasonably Gaussian PSF. For combination with 12M array data, however, this shortcoming of the stand-alone PSF of the 7M array is irrelevant.

5.4 Short observations

In the analysed sample of almost 500 Cycle 6/7 MOUSs from phase 1, we find that for Set 1, 71% of all MOUSs consist of one execution. The on-source time is less than 5 minutes for 7% of the sample and less than 15 minutes for 45% of the sample. Only 21% of all MOUSs have on-source times longer than 1 hour. Also because of these facts, it is important to specially consider short observations when investigating the properties of the ALMA 7M array and the 12M array in all but its most compact configurations. The 7M array and the extended 12M array have too inhomogenous uv coverage for snapshots with high image fidelity. A remedy would be to schedule two snapshot EBs with very different starting hour-angle.

5.5 Observations with no explicit LAS request

Essentially all observations will profit from a good PSF, and so BLD assessment should be carried out on all of them. The computational effort for BLD assessment is small and even if the PI of a particular observation is not interested in high image fidelity, monitoring the BLD of all observations will further help to understand operational constraints.

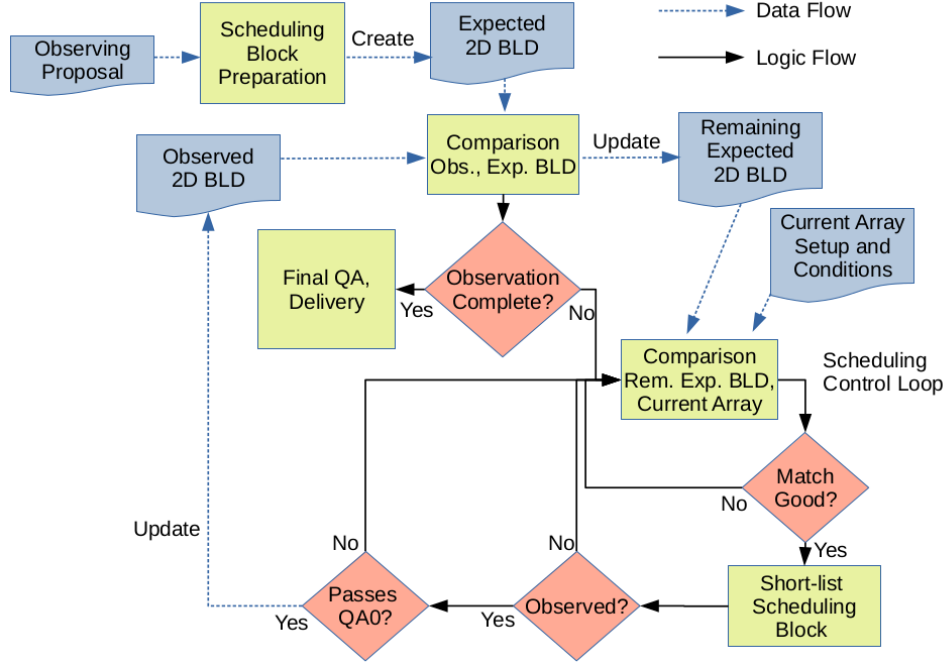


Figure 7. Outline of our proposed new observing control loop with uv coverage tracking via the 2D Baseline Length Distribution (BLD). A scheduling block is preferentially observed when its remaining expected 2D BLD is a good match with the properties of the current array and the general observing conditions.

6. UPDATE TO QUALITY ASSURANCE

We are testing an update to the uv coverage assessment in ALMA QA along the following lines: Based on our analytical expectation, the 4×10 FF matrix should be computed for PSF assessment. Achievement of the AR and overall good PSF Gaussianity is verified by imposing the condition $FF > 0.5$ on all ten BL bins (averaged over azimuth) and on all four azimuthal bins (averaged over BL), i.e. each annulus and each sector in the uv plane should achieve at least 77% of the expected sensitivity.

The necessary low ellipticity of the synthesized beam in all BL ranges is enforced by requiring the FF for each of the ten BL ranges to be approximately constant over the four orientation bins. This homogeneity of the uv coverage in azimuth is measured separately in each BL range by fitting a constant function to the four FF values of the BL range and requiring the χ^2 of the fit to be ≤ 2 . Furthermore, no less than 90% of the elements in the FF matrix must achieve a minimum value of 0.25, i.e. with few exceptions tolerated, each 2D bin in the uv plane should achieve at least 50% of the expected sensitivity.

The achievement of the requested LAS is verified by comparing it to the MRS_L value determined from the observed BLD using our "flat sensitivity" method.

If the above criteria are not fulfilled by an MOUS, a more thorough inspection is warranted.

In a first run on ca. 250 MOUSs from ALMA Cycle 9 12M observations, ca. 50% of the MOUSs did indeed pass this test, 40% showed only minor defects (individual FF matrix bins below 0.25 or individual BL bins being inhomogenous in azimuth) while the remaining 10% had defects like whole sectors or whole annuli having a $FF < 0.5$. In other words, 90% of the ALMA 12M data had a uv coverage with minor or no defects. These numbers show that we are close to the right parameter range for creating QA criteria which ALMA can fulfill but which are still sufficiently ambitious.

7. IMPLICATIONS FOR SCHEDULING

The 7M array and the more extended 12M array configurations need Earth-rotation in order to achieve good coverage of all baseline orientations. Our proposed 2D QA procedure (see above) will detect cases where additional observations at different starting hour-angles (HA) are needed.

Scheduling multi-EB observations will profit from an intermediate uv coverage assessment when an MOUS cannot be completed in one session. We recommend to inspect the so-far achieved HA coverage during the initial per-EB quality assessment (QA0) and schedule the remaining EBs to extend the HA coverage as much as possible with the remaining EBs.

In the ideal case, scheduling should keep track of the 2D BLD achieved so far in order to determine which array setup and which starting HA is best to complete the MOUS and achieve a near-ideal BLD. In Fig. 7 we sketch how the observing control loop could be set up.

As part of this refactoring, the overall "execution fraction" scheme, which is presently in use in ALMA scheduling and QA, would be replaced by one using our 4×10 EF matrix.

8. SOFTWARE DEVELOPED BY THIS STUDY

We have developed a prototype for an ALMA uv coverage assessment tool named "assess_ms" and a number of Python modules for generating BLDs, operating on them, and analysing their properties. After "assess_ms" has been introduced in ALMA science operations and stood the test of a complete ALMA observing cycle, we are planning to make it publicly available for general ALMA users, in particular in the context of data combination.

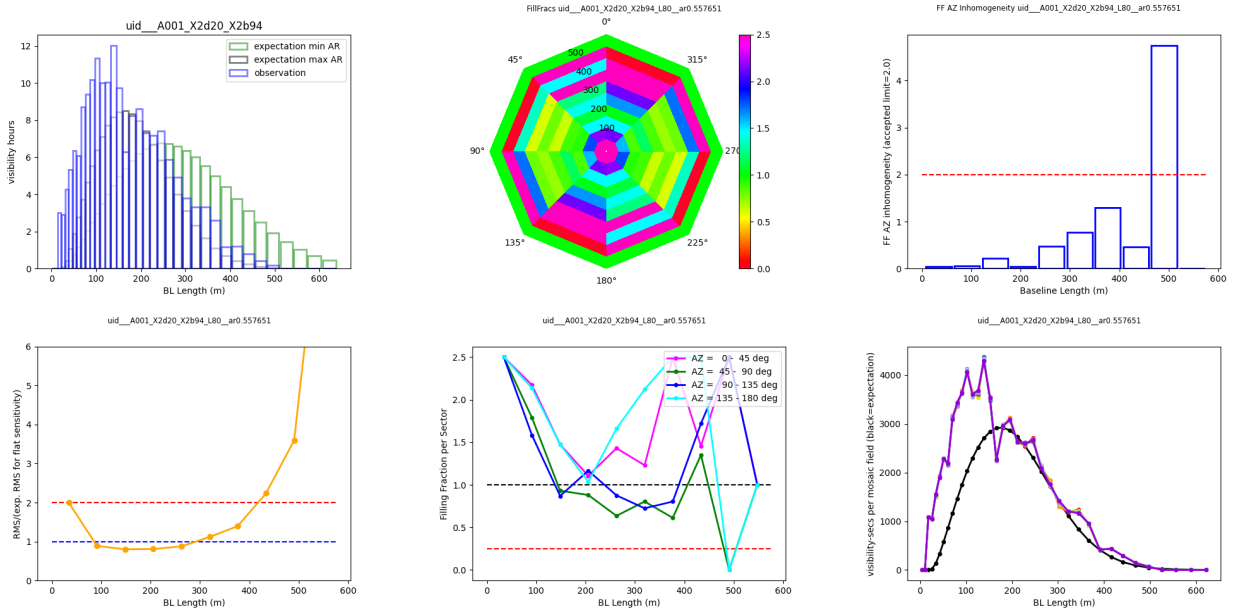


Figure 8. Example of the set of diagnostic plots for uv coverage assessment produced by our analysis tool "assess_ms" for an ALMA observation (a mosaic) with some underexposure at long baselines in two sectors but otherwise good uv coverage: From left to right, first row: comparison of observed BLD with the two expectations for minimal and maximal acceptable AR, 2D Filling Fraction plot, azimuthal inhomogeneity vs. BL (for the BL bin around 500 m, the inhomogeneity measure is above the threshold of 2.0). - Second row: "flat sensitivity" plot (see text), FF vs. BL for each of the four sectors, BLDs for each of the mosaic fields overlotted (with the expected shape for best PSF in black).

ACKNOWLEDGMENTS

We would like to thank Carlos de Breuck (ESO) for his support as the contact person for this ESO ALMA internal development study.

REFERENCES

- [1] Cortes, P. C., Vlahakis, C., Hales, A., Carpenter, J., Dent, W., Kamenon, S., Loomis, R., Vila-Vilaro, B., Immer, K., Law, J., Stoehr, F., and Saini, K., [*ALMA Technical Handbook Cycle 11*], ALMA Doc. 11.3, ver. 1.4 (2024). <https://almascience.eso.org/documents-and-tools/cycle11/alma-technical-handbook>.
- [2] Petry, D., Trigo, M. D., Kneissl, R., Toledo, I., and Facchini, S., “New methods for alma angular-scale based observation scheduling, quality assessment, and beam shaping,” *Proceedings of the SPIE, Volume 11449, id. 114491D 12 pp. (2020)* **11449**(114491D) (2020).
- [3] CASA Team, Bean, B., Bhatnagar, S., Castro, S., Donovan Meyer, J., Emonts, B., Garcia, E., Garwood, R., Golap, K., Gonzalez Villalba, J., Harris, P., Hayashi, Y., Hoskins, J., Hsieh, M., Jagannathan, P., Kawasaki, W., Keimpema, A., Kettenis, M., Lopez, J., Marvil, J., Masters, J., McNichols, A., Mehringer, D., Miel, R., Moellenbrock, G., Montesino, F., Nakazato, T., Ott, J., Petry, D., Pokorny, M., Raba, R., Rau, U., Schiebel, D., Schweighart, N., Sekhar, S., Shimada, K., Small, D., Steeb, J.-W., Sugimoto, K., Suoranta, V., Tsutsumi, T., van Bemmell, I. M., Verkouter, M., Wells, A., Xiong, W., Szomoru, A., Griffith, M., Glendenning, B., and Kern, J., “CASA, the Common Astronomy Software Applications for Radio Astronomy,” *PASP* **134**, 114501 (Nov. 2022).
- [4] Paneque-Carreño, T., Miotello, A., van Dishoeck, E., Tabone, B., Izquierdo, A., and Facchini, S., “Directly tracing the vertical stratification of molecules in protoplanetary disks,” *A&A* **669**, 527 (2023).
- [5] Tsukui, T., Iguchi, S., Mitsuhashi, I., and Tadaki, K., “Estimating the statistical uncertainty due to spatially correlated noise in interferometric images,” *Journal of Astronomical Telescopes, Instruments, and Systems* **9**, 8001 (2023).
- [6] Radcliffe, J., Beswick, R., Thomson, A., and Muxlow, T., “Revisiting a flux recovery systematic error arising from common deconvolution methods used in aperture-synthesis imaging,” *Monthly Notices of the Royal Astronomical Society* **527**, 942 (2023).
- [7] Boone, F., “Weighting interferometric data for direct imaging,” *Experimental Astronomy* **36**, 77 (2013).
- [8] Woody, D., [*Radio Interferometer Array Point Spread Functions II. Evaluation and Optimisation*], ALMA Memo 390 (2001). <http://library.nrao.edu/public/memos/alma/main/memo390.pdf>.
- [9] Hobson, M. P. and Maisinger, K., “Maximum-likelihood estimation of the cosmic microwave background power spectrum from interferometer observations,” *MNRAS* **334**, 569–588 (Aug. 2002).
- [10] Remijan, A., Biggs, A., Cortes, P., Dent, B., Mason, B., Philips, N., Saini, K., Stoehr, F., Vila-Vilaro, B., and Villard, E., [*ALMA Technical Handbook Cycle 7*], ALMA Doc. 7.3, ver. 1.1 (2019). <https://almascience.eso.org/documents-and-tools/cycle7/alma-technical-handbook>.